

**UCLA**

**UCLA Previously Published Works**

**Title**

Mechanical and Biochemical Stimulation of 3D Multilayered Scaffolds for Tendon Tissue Engineering

**Permalink**

<https://escholarship.org/uc/item/1wn9n0pt>

**Journal**

ACS Biomaterials Science & Engineering, 5(6)

**ISSN**

2373-9878

**Authors**

Rinoldi, Chiara  
Fallahi, Afsoon  
Yazdi, Iman K  
[et al.](#)

**Publication Date**

2019-06-10

**DOI**

10.1021/acsbomaterials.8b01647

Peer reviewed

# Mechanical and Biochemical Stimulation of 3D Multilayered Scaffolds for Tendon Tissue Engineering

Chiara Rinoldi,<sup>†,‡,§</sup> Afsoon Fallahi,<sup>‡,§,||</sup> Iman K. Yazdi,<sup>‡,§,||</sup> Jessica Campos Paras,<sup>‡,§,⊥</sup> Ewa Kijeńska-Gawrońska,<sup>†</sup> Grissel Trujillo-de Santiago,<sup>‡,§,⊥</sup> Abuduwaili Tuoheti,<sup>#</sup> Danilo Demarchi,<sup>#</sup> Nasim Annabi,<sup>‡,§,¶</sup> Ali Khademhosseini,<sup>\*,‡,§,||,▽,○</sup> Wojciech Swieszkowski,<sup>\*,†</sup> and Ali Tamayol<sup>\*,‡,§,||,◆</sup>

<sup>†</sup>Materials Design Division, Faculty of Materials Science and Engineering, Warsaw University of Technology, 141 Woloska Street, Warsaw 02-507, Poland

<sup>‡</sup>Biomaterials Innovation Research Center, Department of Medicine, Brigham and Women's Hospital, Harvard Medical School, 65 Landsdowne Street, Boston, Massachusetts 02139, United States

<sup>§</sup>Harvard-MIT Division of Health Sciences and Technology, Massachusetts Institute of Technology, 65 Landsdowne Street, Cambridge, Massachusetts 02139, United States

<sup>||</sup>Wyss Institute for Biologically Inspired Engineering, Harvard University, 3 Blackfan Circle, Boston, Massachusetts 02115, United States

<sup>⊥</sup>Centro de Biotecnología-FEMSA, Tecnológico de Monterrey, Ave. Eugenio Garza Sada 2501 Sur Col. Tecnológico, Monterrey, Nuevo Leon CP 64849, Mexico

<sup>#</sup>Department of Electronics and Telecommunications, Politecnico di Torino, 24 Corso Duca degli Abruzzi, Turin 10129, Italy

<sup>¶</sup>Department of Chemical Engineering, Northeastern University, 360 Huntington Avenue, Boston, Massachusetts 02115, United States

<sup>▽</sup>Center of Nanotechnology, King Abdulaziz University, Jeddah 21569, Saudi Arabia

<sup>○</sup>Department of Chemical and Biomolecular Engineering, Department of Bioengineering, and Department of Radiology, California NanoSystems Institute (CNSI), University of California, 405 Hilgard Avenue, Los Angeles, California 90095, United States

<sup>◆</sup>Department of Mechanical and Materials Engineering, University of Nebraska, 900 N. 16th Street, Lincoln, Nebraska 68588, United States

## Supporting Information

**ABSTRACT:** Tendon injuries are frequent and occur in the elderly, young, and athletic populations. The inadequate number of donors combined with many challenges associated with autografts, allografts, xenografts, and prosthetic devices have added to the value of engineering biological substitutes, which can be implanted to repair the damaged tendons. Electrospun scaffolds have the potential to mimic the native tissue structure along with desired mechanical properties and, thus, have attracted noticeable attention. In order to improve the biological responses of these fibrous structures, we designed and fabricated 3D multilayered composite scaffolds, where an electrospun nanofibrous substrate was coated with a thin layer of cell-laden hydrogel. The whole construct composition was optimized to achieve adequate mechanical and physical properties as well as cell viability and proliferation. Mesenchymal stem cells (MSCs) were differentiated by the addition of bone morphogenetic protein 12 (BMP-12). To mimic the natural function of tendons, the cell-laden scaffolds were mechanically stimulated using a custom-built bioreactor. The synergistic effect of mechanical and biochemical stimulation was observed in terms of enhanced cell viability, proliferation, alignment, and tenogenic differentiation. The results suggested that the proposed constructs can be used for engineering functional tendons.

**KEYWORDS:** tendon tissue engineering, composite scaffolds, nanofibrous materials, mechanical stimulation, stem cell differentiation



## INTRODUCTION

Tendons are organized connective tissues that transfer forces generated by skeletal muscles to bones in order to move them. Meanwhile, they withstand high stress from muscle contractions

**Received:** December 28, 2018

**Accepted:** April 16, 2019

**Published:** April 16, 2019

and avoid overloading bones. Thus, tendons are essential in the normal movement of the body. They are highly organized tissues, which are comprised of aligned, multiscale, and hierarchical collagen fibers.<sup>1</sup> Due to their structure, tendons are capable of carrying loads, supporting and stabilizing the joint while preventing bone dislocation.<sup>2</sup> Tendon injuries arise mostly from high-pivoting sporting activities such as skiing, basketball, and football. Additionally, degenerative tissue processes occur quite often, mainly in the middle-aged and elderly population.<sup>3</sup> However, the low number of cells and low blood supply to tendons reduce their regenerative and reparative capability.<sup>4</sup> Clinical treatments of tendon injuries are based on surgical suturing of damaged tendons as well as the use of auto- and allografts.<sup>5</sup> These surgical procedures are associated with a number of major challenges including the lack of a sufficient number of auto- and allografts, the significant chance of rejection of allografts, and infections.<sup>6</sup> Because of these reasons, engineered biological substitutes with biomimetic, mechanical, and biological properties have attracted noticeable attention to replace or repair injured tendons.<sup>7</sup>

Various strategies are devised for the production of scaffolds with biomimetic architectures and anisotropic mechanical properties for tendon tissue engineering. Fiber-based approaches including weaving, knitting, braiding, and electrospinning have been widely explored for engineering fibrous structures with adequate mechanical properties.<sup>8</sup> Among them, electrospinning and braiding have been more successful and popular in generating highly organized fibrous constructs with anisotropic mechanical properties.<sup>9,10</sup> Electrospinning allows the production of very fine fibers in the range of 100 nm to a few micrometers by flowing a polymer solution through a needle placed in an electric field.<sup>11</sup> Nanofibrous scaffolds offer some unique advantages such as large specific surface area and high porosity. Furthermore, the electrospinning technique could be used for the production of aligned and organized nanofibrous scaffolds, recapitulating the collagen fiber direction structure of anisotropic tissues and directing the cell adhesion.<sup>12</sup> Due to these great advantages, electrospun nanofibrous scaffolds have been successfully applied to musculoskeletal tissues including bone, cartilage, tendon, ligament, annulus fibrosus, and tendon.<sup>13–18</sup> Even though it has been proven that synthetic fibrous electrospun structures can mimic the native extracellular matrix (ECM),<sup>19</sup> they cannot provide a suitable 3D micro-environment for cell attachment, proliferation, migration, and differentiation due to the lack of cell-recognition sites.<sup>20</sup> Recently, engineered composite and multicompartiment fibers, followed by their braiding, enabled the engineering of centimeter-scale constructs. The braided constructs encapsulated cells in a cell-supporting hydrogel niche where they can easily remodel and populate the entire structure, while the mechanical properties of the construct are tailored by the polymeric component of the scaffolds.<sup>21–25</sup>

Some of the natural-based hydrogels have cell binding and matrix metalloproteinase responsive motifs; as a result, cells can spread and proliferate.<sup>26</sup> For example, recent studies demonstrated that tendon-derived ECM allows high cell infiltration as well as collagen deposition and that methacryloyl gelatin (GelMA) permits homogeneous cell distribution and penetration.<sup>27,28</sup> Thus, the physicochemical and biological properties of the hydrogel play a key role on the growth and function of the encapsulated cells.<sup>29</sup>

In addition to creating a suitable scaffold, the selection of cell sources has also been the subject of various studies. Among

different cell sources for bone and tendon regeneration studies, mesenchymal stem cells (MSCs) have been frequently used due to their natural tendency to differentiate into these lineages.<sup>30–32</sup> Biochemical stimulation of the cultures using growth factors (GFs) that can potentially induce tenogenic differentiation has been introduced to overcome the disadvantages of stem cell therapies. Indeed, even though stem cell application is considered as the ideal approach for clinical translation, specific methods for inducing tenogenic differentiation are still undiscovered. Biomechanical stimulations performed by different GFs, such as basic fibroblast GF,<sup>33</sup> platelet-derived growth factor BB,<sup>34</sup> transforming GF beta,<sup>35,36</sup> bone morphogenic proteins (BMPs),<sup>37,38</sup> and growth differentiate factor 5,<sup>39</sup> have been lately considered to induce the tendon regeneration. GFs can be supplied by addition into the culture media composition, as well as by loading of the bioactive molecules into the scaffolds structure, i.e., incorporation into electrospun fibers or encapsulation into nanoparticles. It has been demonstrated that GF treatment plays the main role in the chemical cellular stimulation and in the tissue homeostasis, healing, and repair, affecting cell proliferation, morphology and migration, collagen production, angiogenesis, and deposition of ECM proteins.<sup>38,40</sup>

In particular, BMPs are considered crucial in skeletal tissue development, because of their influence on osteogenic or chondrogenic differentiation.<sup>41</sup> In particular, it has been demonstrated that bone morphogenetic protein 12 (BMP-12) causes a tenogenic pathway in stem cells, up-regulating key tenogenic transcription factors and causing significant changes in the cell secretory activity, enhancing the secretion of VEGF and collagenases, which might improve the regeneration process in acute tendon injuries.<sup>42,43</sup> Thus, BMP-12 has been pointed out as promising for accelerating tendon healing.<sup>44,45</sup> The mechanisms of BMP-12 on improving tenogenic differentiation are probably induced by activating cytoskeleton reorganization signaling or activating the Smad1/5/8 signaling pathway.<sup>46</sup> *In vitro* studies of BMP-12 treatment of canine adipose derived stem cells results in higher specific tenogenic gene expression, such as scleraxis and tenomodulin, proving its potential for tenogenic cell differentiation compared to untreated conditions.<sup>37</sup> Moreover, the implantation of human BMP-12 loaded into an absorbable collagen sponge was reported to enhance the healing of rotator cuff injuries in 87% of patients at a 1-year follow-up.<sup>47</sup> Additionally, the injection of BMP-12 in the Achilles tendon in a mouse animal model proved to improve the quality of tendon repair.<sup>48</sup>

The dynamic culture condition of the scaffolds has recently demonstrated its potential for a more efficient tissue maturation. In particular, bioreactor systems have been developed in order to recapitulate the tissue natural conditions *in vivo*.<sup>49</sup> In the case of tendon tissue, different bioreactor devices that can apply periodic physiological mechanical stretching have been proposed. The mechanical stimulation of the cultures resulted in an improvement of cell proliferation rate<sup>50</sup> and the formation of highly oriented cellular architecture,<sup>51</sup> which is essential for the proper function of tendons. Moreover, a positive effect of the mechanical stretching on tenogenic differentiation of stem cells has also been reported.<sup>35,38</sup>

In this work, multilayered (ML) scaffolds based on electrospun substrates coated with layers of cell-laden hydrogel are explored for tendon tissue engineering. In the final scaffold, the fibrous membrane provides the adequate mechanical properties and the hydrogel layers mimic the ECM environment, facilitating cell spreading and three-dimensional growth.<sup>52</sup> The

biochemical and mechanical stimulations of the construct were selected to create an *in vitro* model, which performs dynamic cell culture and reproduces the tendon physiological conditions. The influence of the scaffold composition and mechanical and biochemical stimuli has been investigated.

## MATERIALS AND METHODS

**Materials.** All the chemicals including polycaprolactone (PCL,  $M_n$  80 000), nylon-6 (PA6), hexafluoroisopropanol (HFIP), high viscosity alginate (Alg), methacrylic anhydride, gelatin (Type A, 300 bloom from porcine skin), 2-hydroxy-4'-(2-hydroxyethoxy)-2-methylpropionone (Irgacure 2959), ascorbic acid, Triton X-100, and bovine serum albumin (BSA) were purchased from Sigma-Aldrich (St. Louis, MO, USA). Primary human bone marrow derived mesenchymal stem cells (MSCs) were purchased from Roosterbio Inc. (Frederick, MD, USA). The cells were isolated and expanded from a single deidentified human donor bone marrow. Minimum essential medium alpha ( $\alpha$ -MEM), fetal bovine serum (FBS), phosphate buffer solution (PBS), basic fibroblast growth factor (bFGF), trypsin-EDTA, L-glutamin, collagen I monoclonal antibody, Alexa Fluor 488 Phalloidin, and DAPI were obtained from Life Technologies (Carlsbad, CA, USA). BMP-12 was bought from BioVision, Inc. (Mountain View, CA, US).

**Biofabrication Methods. Electrospinning of Nanofibrous Membranes.** PCL-PA6 nanofibrous membranes were fabricated using a conventional electrospinning setup. Briefly, 10% (w/v) PCL and 10% (w/v) PA6 were separately dissolved in HFIP. The solutions were mixed in a 1:1 ratio in order to obtain a homogeneous polymeric blend of 5–5% (w/v) PCL-PA6 solution. The PCL-PA6 prepolymer solution was then transferred to a 3 mL syringe with a 23G blunt needle tip. An electrical field of 15 kV over a fixed spinning distance of 20 cm was applied. The flow rate of the prepolymer solution was set at 1 mL/h, and the substrates were spun for 30 min to generate fibrous membranes. Fibers were collected onto an aluminum flat collector to produce a sheet with uniform fiber distribution. The membrane was vacuum-dried for 24 h and then sterilized under UV light overnight.

**Hydrogel Formulation and Preparation.** GelMA was synthesized as previously described.<sup>27</sup> Briefly, type A porcine skin gelatin was dissolved in PBS at 50 °C in a concentration of 10% (w/v) and stirred at 240 rpm. Subsequently, 5% (v/v) of methacrylic anhydride was added dropwise (0.5 mL/min) and stirred at 50 °C for 3 h. Afterward, 300% (v/v) of PBS was used to dilute the gelatin solution. The final solution was loaded in dialysis membranes (Spectro/Por molecular porous membrane tubing, MWCO 12–14 000, Fisher Scientific) and dialyzed in 5 L of distilled water at 60 °C and 500 rpm for 10 days. Finally, the solution was freeze-dried to obtain lyophilized GelMA.

A GelMA 20% (w/v) solution was prepared by dissolving lyophilized GelMA in PBS at 80 °C containing 0.2% (w/v) of Irgacure 2959 as the photoinitiator. Alg solutions of 1%, 2%, and 3% (w/v) were prepared by dissolving the polymer powder in deionized water at room temperature overnight. The final solutions were prepared by mixing GelMA and Alg solutions (1:1 ratio) in order to obtain GelMA-Alg solutions of 10%–0.5% (w/v), 10%–1% (w/v), and 10%–1.5% (w/v), respectively. Finally, the solutions were filtered through a 0.22  $\mu$ m pore size sterilizing filter.

**Fabrication of ML Scaffolds.** The electrospun membrane surfaces were subjected to plasma treatment for 45 s and then coated with a ~100–150  $\mu$ m layer of GelMA-Alg composite hydrogel. The dip-coating method was used to coat a thin layer of hydrogel on the fibrous surfaces. The hydrogel was cross-linked first in a 2% (w/v) sterile calcium chloride ( $\text{CaCl}_2$ ) bath for 20 s, and subsequently, photopolymerization was carried out by UV light exposure at 800 mW  $\text{cm}^{-2}$  for 30 s (Omnicure, S2000, 360–480 nm, Excelitas Tech. Corp., US).<sup>27</sup>

**Morphology Evaluation.** The morphology of ML scaffolds was investigated using a scanning electron microscope (SEM; Zeiss Ultra Plus). SEM images were acquired at 7 kV after coating the samples with a thin layer of gold using a sputter coater. The diameter of the fibers was evaluated from SEM images using ImageJ (National Institute of Health, USA) by measuring the dimensions of 100 randomly selected fibers on five independent samples.

**Mechanical Characterization. Tensile Test.** The mechanical properties of the constructs were measured through a uniaxial tensile strength test using a universal mechanical testing machine (Instron 5542, Norwood, MA). Five samples of each membrane were cut in a rectangular shape (10 mm  $\times$  5 mm), positioned between the two grips of the machine, and subjected to tensile mechanical stretching. The constant crosshead speed was set at 10 mm/min, and the related force was measured using a 10 N cell. Tensile modulus of elasticity was calculated using the initial 0–5% linear region of the stress–strain curve.

**Compression Test.** Compressive mechanical properties of the scaffolds were measured by a compression test using Instron 5542 (Instron, Norwood, MA, USA). Samples were produced in the form of disks with a diameter of 10 mm, and the compression rate was set to 2 mm/min. The compressive modulus was calculated using the initial 0–5% linear region of the stress–strain curves.

**Physical Characterization. Swelling Assessment.** Fluid handling capacity was measured by soaking the samples in 2 mL of PBS. The weight before and after immersion in the solution was measured with a high precision scale to assess the swelling ratio every day up to 7 days. The swelling ratio was calculated on the basis of eq 1.

$$\text{swelling ratio\%} = \frac{W_f - W_i}{W_i} \times 100 \quad (1)$$

where  $W_f$  is final weight and  $W_i$  is initial weight.

**Degradation Profile.** The degradation rate of the constructs was evaluated by placing the samples in 2 mL of PBS at 37 °C. The dry weight of the specimens was measured before the experiment and then after 7 and 14 days of incubation using a high precision scale. The weight loss percentage was calculated on the basis of eq 2.

$$\text{weight loss\%} = \frac{W_{fd} - W_{id}}{W_{id}} \times 100 \quad (2)$$

where  $W_{fd}$  is dry final weight and  $W_{id}$  is dry initial weight.

**Cell Studies.** MSCs were cultured in growth culture media composed of alpha MEM supplemented with 10% FBS, 0.2 mM ascorbic acid, 2 mM L-glutamin, 1% penicillin–streptomycin (PS), and 1 ng/mL bFGF until sufficient confluence was obtained.<sup>53</sup> Further, cells were detached using trypsin-EDTA, encapsulated in the hydrogel structures at a density of  $3 \times 10^6$  cell/mL, and cultured at 37 °C and 5%  $\text{CO}_2$  for 14 days. The two-dimensional (2D) culture control condition was also assessed, seeding MSCs on culture plates and culturing them at 37 °C and 5%  $\text{CO}_2$  for 14 days.

**Cell Proliferation Assessment.** The PrestoBlue assay was performed to evaluate cell proliferation. The samples were treated with 10% (v/v) of PrestoBlue solution in the culture medium solution and incubated at 37 °C and 5%  $\text{CO}_2$  for 1.5 h. The resulted solution was aliquoted in 100  $\mu$ L aliquots and transferred to a 96 well plate. The fluorescence intensity was measured using a BioTek Synergy 2 multimodal plate reader (BioTek Instruments Inc., VT, US).

**Cell Viability Assessment.** Cell viability was determined using a LIVE/DEAD Cell Viability Kit (Invitrogen) to evaluate the response of cells cultured on the scaffolds.<sup>54</sup> At each time point, the constructs were washed in PBS and treated with 0.5  $\mu$ L/mL calcein and 2  $\mu$ L/mL ethidium homodimer in PBS. The first compound was used for the green staining of alive cells and the second, for the red staining of dead cells. Samples were incubated for 10 min at 37 °C and 5%  $\text{CO}_2$ . Afterward, the samples were washed in PBS and imaged with a fluorescent microscope (AxioCam MRcS, Carl Zeiss, Germany).

**Cell Morphology and Alignment Characterization.** Cell morphology and alignment were evaluated by staining cell cytoskeletons and nuclei. Actin-DAPI staining was performed. Samples were treated with 4% paraformaldehyde for 30 min and then washed in PBS 3 times (5 min each). Subsequently, 0.3% (v/v) Triton X-100 in PBS was added for 15 min, and three washing steps were performed. Samples were incubated in 1% (w/v) BSA in PBS for 30 min, and a 1:40 dilution of Alexa Fluor phalloidin in PBS was added for 40 min at room temperature. Three washing steps were performed. Subsequently, samples were incubated in 1:500 DAPI solution in PBS for 10 min and

Table 1. Polymerase Chain Reaction (PCR) Primer Sequences

gene	forward primer sequence (5' to 3')	reverse primer sequence (5' to 3')
GAPDH	CAAGGCTGAGAACGGGAAGC	AGGGGGCAGAGATGATGACC
TNMD	GATCTTCACTTCCTACCAACG	CTCATCCAGCATGGGGTC
SCX	ACACCCAGCCAAACAGA	GCGGTCCTTGCTCAACTTTC
COL I	GGCTCCTGCTCCTCTTAGCG	CATGGTACCTGAGCCGTTCC
DCR	CGCCTCATCTGAGGGAGCTT	TACTGGACCGGGTTGCTGAA
TNC	GGTGGATGGATTGTCTCTGAGA	CTGTGTCTTGTCAAAGGTGGAGA

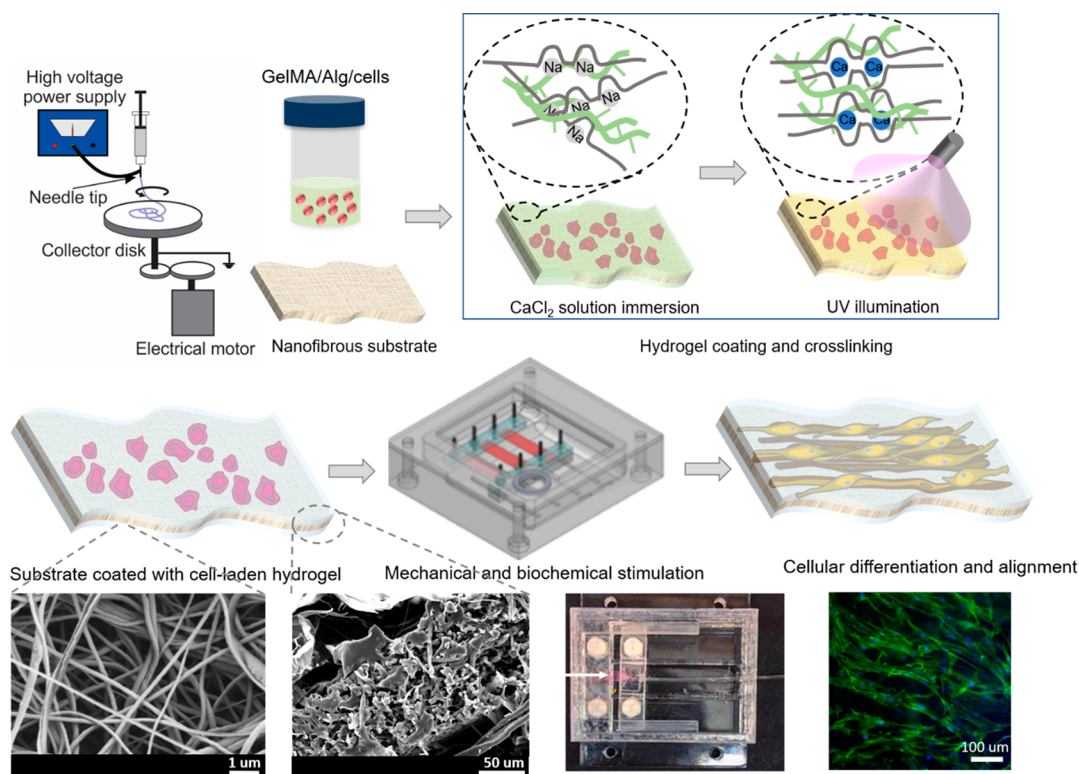


**Figure 1.** Schematic of fabrication and stimulation of ML scaffolds. Synthetic electrospun nanofibers were coated by thin layers of cell-laden hydrogel to fabricate a ML scaffold for tendon tissue engineering. The hydrogel was first cross-linked in a calcium chloride solution and secondarily exposed to UV light. The cell-laden scaffolds were cultured in bioreactors, which allow the administration of GFs and periodic mechanical stretching to promote cell alignment and differentiation. SEM images of nanofibrous substrate and then cross section of the ML scaffold are reported in the bottom row.

washed again. Scaffolds were imaged under the fluorescence microscope (AxioCam MRcS, Carl Zeiss, Germany). Cell alignment was calculated from fluorescence images using ImageJ (National Institute of Health, USA) by measuring the cytoskeletons orientation (ImageJ software, OrientationJ).

**Collagen Expression Analysis.** Collagen I expression was assessed to evaluate the ECM deposition. The cell-laden constructs were washed in PBS and then fixed in 4% (w/v) paraformaldehyde for 30 min. Afterward, three washing steps were performed (5 min each). Subsequently, 0.3% (v/v) Triton X-100 solution in PBS was added for 15 min, and another three washing steps were performed. The nonspecific staining was blocked by incubation in 1% BSA for 30 min at room temperature (RT). Then, the samples were incubated in an anticollagen I antibody produced in mouse solution (1:2000 dilution) overnight. Three washing steps were performed. Subsequently, the scaffolds were incubated in Alexa Fluor 488 goat antimouse secondary antibody produced in goat solution (1:300 dilution) in the darkness at RT for 2 h. After washing the samples, the nuclei were stained with DAPI solution (1:500) and incubated in the darkness for 10 min. Lastly, two washing steps were performed, and samples were visualized using a fluorescence microscope (AxioCam MRcS, Carl Zeiss, Germany).

**Real-Time PCR Analysis.** Electrospun substrate coated cell-laden hydrogels were mechanically disrupted, and TRIzol (Invitrogen, Inc.) was used to extract the total RNA from these samples; total RNA yields

were measured using a NanoDrop (Thermo Scientific). One microgram of total RNA from each sample was reverse transcribed according to the manufacturer's instructions using the SuperScript III First-Strand Synthesis SuperMix (Invitrogen, Inc.). All RT-PCR reactions were prepared using the iTaq Universal SYBR Green Master (Thermo Fisher, USA). The 20  $\mu$ L volume reaction component included 10  $\mu$ L of Master Mix, 1  $\mu$ L of forward and reverse primers, and 100 ng of cDNA template, and the final volume was adjusted using a nuclease free water. Collagen type I, decorin, tenascin-C, scleraxis, and tenomodulin were selected as target gene primers, and they have been listed in Table 1. Relative expressions were calculated using a  $\Delta\Delta C_t$  method and normalized to GAPDH gene expression.

**Biochemical Stimulation.** The evaluation of BMP-12 concentration in the culture media was assessed. Previous studies demonstrate that BMP-12 plays an important role in chemical cellular stimulation as well as in the tissue homeostasis, healing, and repair, affecting cell proliferation and migration, collagen production, angiogenesis, and deposition of ECM proteins.<sup>37,42,55</sup> In order to perform the biochemical stimulation of the cultures, samples were cultured in growth supplemented with BMP-12. Different concentrations of BMP-12, such as 0, 1, and 10 ng/mL, were added to the medium to achieve the most efficient MSC differentiation, spreading, and proliferation and accelerate the tissue healing and remodeling.

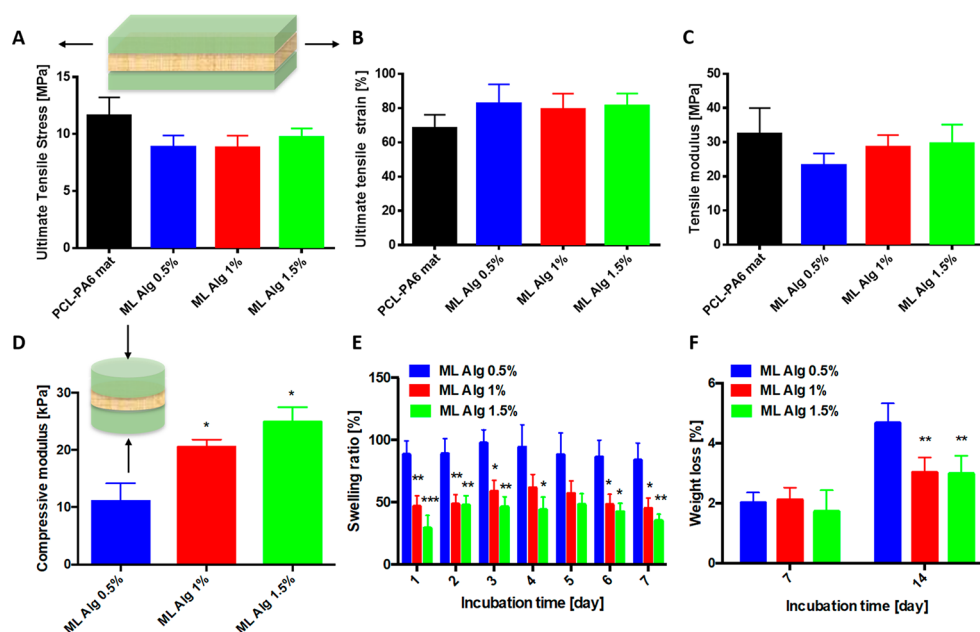


**Figure 2.** Mechanical and physical properties of fibrous ML scaffolds: PCL–PA6 electrospun mat surfaces were coated by 100–150  $\mu\text{m}$  of hydrogel layers. The hydrogel was composed of 10% GelMA and an optimized concentration of Alg. (A–C) Tensile properties of the ML scaffolds are reported in terms of ultimate tensile stress (A), strain (B), and elastic modulus (C) ( $n = 5$ ). No significant influence of the hydrogel coating is reported, showing that the tensile mechanical properties of the PCL–PA6 electrospun construct were maintained. Moreover, the Alg concentration did not influence the tensile characteristic of ML scaffolds in terms of tensile stress ( $\sim 10$  MPa), strain ( $\sim 80\%$ ), and elastic modulus ( $\sim 30$  MPa). (D) The compressive modulus of ML constructs was considerably affected by the Alg concentration, showing significantly higher values of up to 27 kPa for 10%–1% and 10%–1.5% GelMA–Alg hydrogel compositions compared to the lowest Alg concentration tested ( $n = 5$ ). Swelling ratio (E) and weight loss (F) values were measured to be significantly higher for the ML samples with the lowest Alg content (10%–0.5% GelMA–Alg), compared to the samples with higher Alg concentration ( $n = 5$ ). No significant difference was registered between ML scaffolds composed of 10%–1% and 10%–1.5% GelMA–Alg hydrogels. Significant differences are determined compared to the ML 10%–0.5% GelMA–Alg condition ( $*p < 0.05$ ,  $**p < 0.01$ ,  $***p < 0.001$ ,  $****p < 0.0001$ ).

**Mechanical Stimulation: Bioreactor Model.** A bioreactor model was designed and developed to perform the dynamic cell culture on the proposed scaffolds. The bioreactor system has the potential to provide an appropriate biochemical and biomechanical environment to stimulate cell proliferation and differentiation as well as ECM synthesis under sterile conditions. The bioreactor device was designed to hold different samples (ranging in size from 5 to 37 mm in length, 0.2 to 13.5 mm in width, and 0.1 to 2 mm thick) between one fixed grip and one moving grip, which was connected to a pulley through a polymer wire. The pulley was rotated by a stepper motor controlled by a Raspberry PI embedded system (Figure S1). Mechanical stimulation parameters were selected in terms of strain and frequency to simulate the tendon native biochemical conditions.<sup>56,57</sup> The mechanical simulation was performed by periodically stretching the samples in the axial direction. Constructs were subjected to 10% strain with a frequency of 1 Hz for 7 days (4 h/day).

**Statistical Analysis.** All measurements were made in triplicates on at least three different samples produced from different cell cultures and tested independently. Data is reported as mean values  $\pm$  standard deviation. The one-way ANOVA test was performed, and differences are displayed as statistically significant when  $p \leq 0.05$ . Statistically significant values are presented as  $*p \leq 0.05$ ,  $**p \leq 0.01$ ,  $***p \leq 0.001$ , and  $****p \leq 0.0001$ .

## RESULTS

In this work, we have designed and fabricated ML scaffolds composed by an electrospun mat coated by thin layers of hydrogel. The engineered composite platform was comprised of multiple compartments that can be independently tailored. The nanofibrous substrate provided the mechanical support to the scaffold while the hydrogel structure emulates the micro-environment and characteristics of the native ECM. The

electrospun substrates were initially soaked in the mixture of GelMA–Alg, and then, the Alg component was cross-linked using  $\text{CaCl}_2$ . The GelMA component was then cross-linked by UV cross-linking. A custom-built bioreactor was designed and assembled in order to apply biological and periodic mechanical stimulation to the constructs. The schematic of the fabrication process and stimulation of the ML scaffolds is shown in Figure 1.

PCL has been approved by the FDA for drug delivery devices, sutures, and adhesion barriers. Moreover, it has been widely used for fabrication of tissue engineering scaffolds.<sup>58,59</sup> PA6 is also a polymer that has been used in biomedical engineering applications due to its mechanical strength, toughness, and slow degradation profile. Nanofibrous substrates were fabricated by electrospinning of PCL–PA6 solutions in HFIP. The electrospinning parameter was adjusted in order to obtain homogeneous, beadless, and regular fibers with diameter of  $149 \pm 32$  nm (Figure 1). The polymer concentration and the electrospinning parameters were optimized to produce electrospun structures which can provide mechanical properties that can support for the proper function of scaffolds designed for the repair of injured sites of tendon tissue. Uniaxial tensile test results showed that the ultimate tensile stress of 5%–5% (w/v) PCL–PA6 substrates was measured at  $\sim 12$  MPa (Figure 2A).

The hydrogel coating did not affect the mechanical tensile properties of the polymeric electrospun constructs. Stress–strain curves of hydrogel coated ML samples were comparable with noncoated structures without any significant effect on the tensile characteristics in terms of ultimate stress, strain, or elastic modulus, demonstrating that the electrospun component provided the mechanical properties of the whole construct

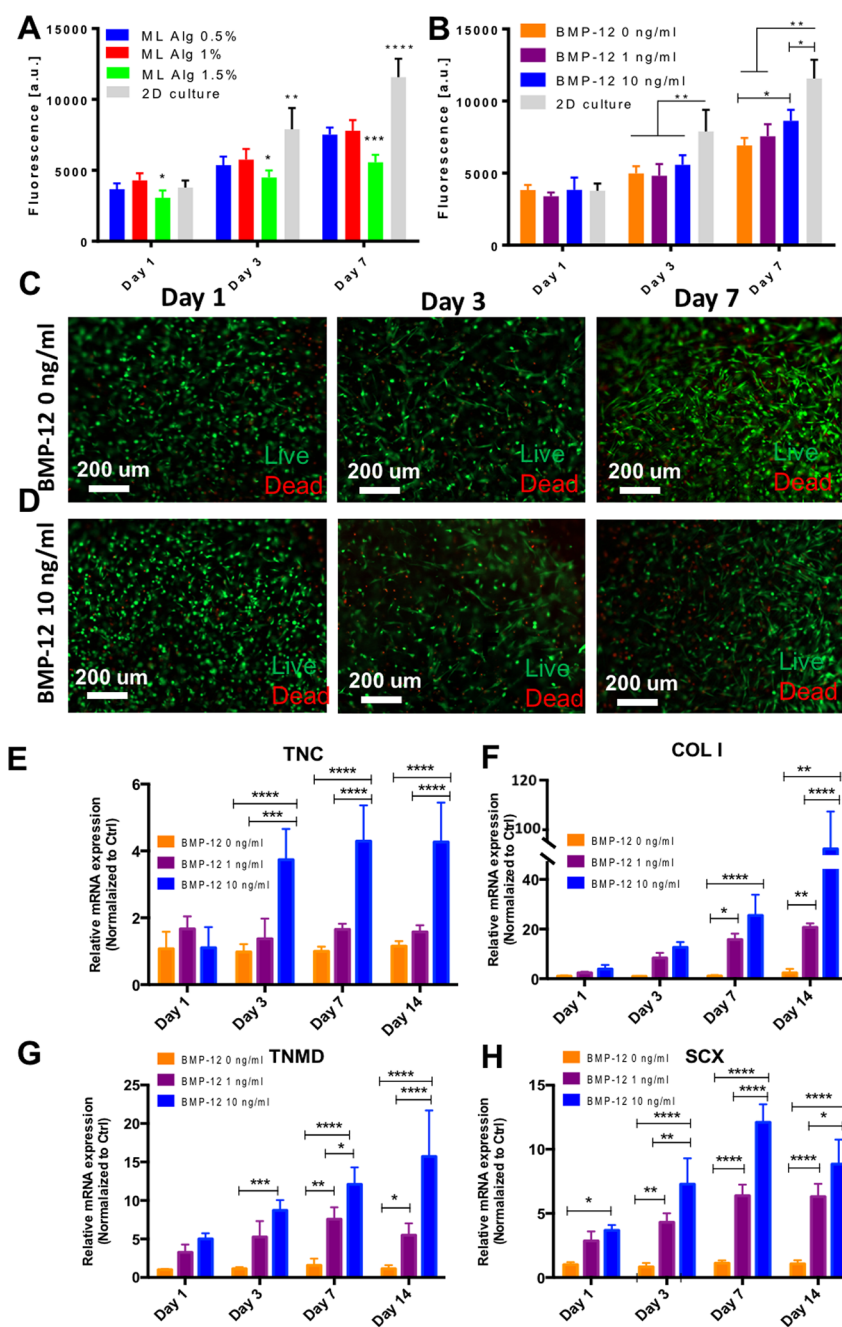


**Figure 3.** Biological performance of fibrous ML scaffolds. The Alg concentration of the hydrogel layers was optimized, and scaffolds were biologically characterized. (A) Cell proliferation increased during the culture time for all tested 2D and 3D conditions except for ML 10%–1.5% GelMA–Alg composition, which appeared to have an inhibitory effect on proliferation ( $n = 5$ ; significant differences are determined compared to the ML 10%–0.5% GelMA–Alg condition). (B) The effect of BMP-12 addition on the cell proliferation of cultured MSCs ( $n = 5$ ). Biochemical stimulation was investigated considering different concentrations of BMP-12 in the culture medium. (C, D) Live/Dead images of MSCs cultured into the ML scaffolds show high cell viability (>96% appeared in green color), spreading, and elongation at each time point without the addition of BMP-12 (C) and in the presence of 10 ng/mL of BMP-12 (D) ( $n = 3$ ). (E–H). The effect of BMP-12 treatment on MSCs tenogenic gene expression was evaluated through PCR analysis of tenascin C (E), collagen I (F), tenomodulin (G), and scleraxis (H) tenogenic marker expression that was significantly higher than the control for 1 (ng/mL) BMP-12 but was maximally expressed for 10 ng/mL BMP-12 concentration in the culture media ( $n = 3$ ). Significant differences: \* $p < 0.05$ , \*\* $p < 0.01$ , \*\*\* $p < 0.001$ , and \*\*\*\* $p < 0.0001$ .

(Figure 2A–C). Moreover, different GelMA–Alg hydrogel compositions containing GelMA 10% (w/v) and Alg 0.5%, 1%, and 1.5% (w/v) did not considerably influence the tensile properties of the scaffolds. However, mechanical compressive properties measured during compression test were significantly affected by the hydrogel composition. ML scaffolds having higher Alg concentration (10%–1% and 10%–1.5% GelMA–

Alg) resulted in higher compressive properties, showing modulus values of up to ~27 kPa (Figure 2D). The swelling ratio of ML scaffolds with three different hydrogel compositions showed a similar trend; softer gels swelled easier. The results suggested that the lower concentrations of Alg (0.5% w/v) resulted in higher swelling ratio of about double the value for those containing Alg 1% (w/v) and Alg 1.5% (w/v) (Figure 2E).

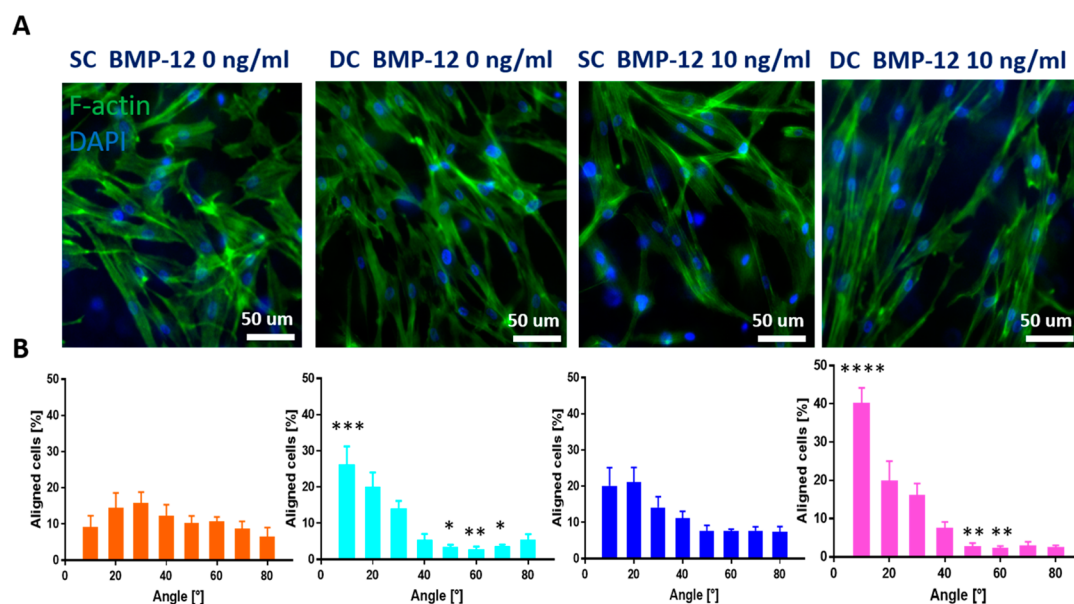


**Figure 4.** Mechanical and biochemical stimulation of fibrous ML scaffolds. (A) Fluorescence images of the cell cytoskeletons after 7 days of culture show cell alignment in the direction of the stretching for the scaffolds mechanically stimulated, while random cell orientation was observed for construct cultured under static conditions. (B) The alignment of MSCs within the ML scaffolds was quantified, reporting that cells dynamically cultured and chemically stimulated can align up to 40% in the direction of the strain ( $n = 3$ ; significant differences are determined compared to the SC BMP-12 0 ng/mL condition: \* $p < 0.05$ , \*\* $p < 0.01$ , \*\*\* $p < 0.001$ , and \*\*\*\* $p < 0.0001$ ).

Figure 2F illustrates that the 10%–0.5% (w/v) GelMA–Alg ML scaffold performed the fastest degradation rate, losing ~5% of the initial dry weight in 14 days, while ML structures with higher Alg concentration such as 10%–1% (w/v) and 10%–1.5% (w/v) GelMA–Alg formed scaffolds more resistant to *in vitro* degradation conditions.

In order to test the biological properties of the scaffolds, MSCs were encapsulated into the hydrogel structures and deposited on the electrospun membranes. The proliferation of the cells up to 7 days is reported in Figure 3A,B. The graphs show a linear growth of the cells during the culture time for all tested conditions. However, after 3 days of culture, cells cultured in 2D have a higher proliferation rate than cells cultured into 3D constructs. This is probably due to the flat cell-friendly tissue culture substrate, which is well-known to allow easy and efficient cell attachment, signaling, and proliferation.<sup>60</sup> However, in Figure 3A, it is possible to visualize that the proliferation of cells cultured into ML scaffolds composed of 10%–1.5% (w/v) GelMA–Alg hydrogel appeared to be inhibited. Cellular growth and proliferation was significantly higher in hydrogels containing lower Alg concentration due the formation of stiffer and denser hydrogels at higher concentrations of Alg, which did not favor cell migration, spreading, and proliferation.<sup>61</sup> Fluorescence images of the representative MSCs cultured into the ML scaffold constructs after Live/Dead staining, where live cells appear green while nonviable cells are stained in red, demonstrated that the majority of the cells were alive (>94%), spread, and elongated. There was not an evident difference that could be visualized between different hydrogel compositions (Figure S2). Considering the mechanical and physical properties of different hydrogel composition and their effect on cellular proliferation, ML scaffold composed of an electrospun mat coated by 10%–1% (w/v) GelMA–Alg hydrogel layers was selected and used for the rest of the study.

Biochemical stimuli were applied to promote and favor the tenogenic differentiation of MSCs encapsulated within the ML

constructs. BMP-12 was selected as a GF to influence the cell fate into tenocyte lineage. A concentration of BMP-12 into the culture medium was selected to stimulate the cells toward tenogenic differentiation. BMP-12 solutions at different concentrations (0, 1, and 10 ng/mL) were tested. Cells proliferated linearly during the culture time for all the tested concentrations (Figure 3B). Among 3D conditions, a significant increase of cell proliferation was registered at day 7 when 10 ng/mL of BMP-12 was added into the medium. The viability of the cells cultured for 7 days into the scaffold is shown in Figures 3C,D and S2. The Live/Dead Cell Viability Assay results suggested that the majority of cells were alive up to 7 days of culture in modified media (>96%), proving that the selected BMP-12 concentrations were not cytotoxic.

To identify the role of BMP-12 on stem cell differentiation, the expression of key tenogenic markers such as tenomodulin, collagen I, scleraxis, and tenascin C was assessed (Figure 3E–H). At early stages, the tenogenic gene expression showed no significant difference for any of the BMP-12 concentrations tested (with the exception of the scleraxis marker). However, from day 3 of culture, an important enhancement of the tenogenic marker expression was detected at each time point in the presence of BMP-12. A treatment with 10 ng/mL of BMP-12 showed a clear improvement on gene expression in terms of tenomodulin, collagen I, tenascin C, and scleraxis markers compared to the untreated condition, suggesting the positive role of BMP-12 in inducing tenogenic differentiation of MSCs. The addition of 10 ng/mL of BMP-12 into the culture medium appeared to simultaneously improve cell proliferation and differentiation. We speculate that this trend was due to the lack of differentiation of MSCs to mature tenocytes, which did not affect the cell division cycle. Thus, a 10 ng/mL concentration of BMP-12 into the culture medium was selected, and the biochemical stimulation of the construct was performed using that composition.

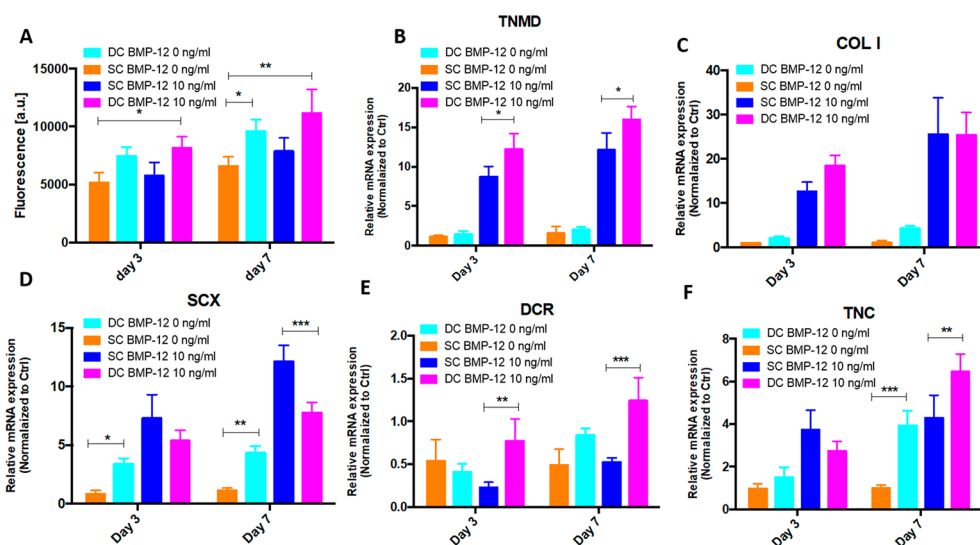


**Figure 5.** Mechanical and biochemical stimulation effects on MSCs encapsulated into ML scaffolds. (A) Proliferation rate of MSCs was registered to be significantly improved by the combination of the mechanical and biochemical stimuli at each time point ( $n = 3$ ). (B–F) Data representing Rt-PCR of mRNA expression of tenomodulin (B), collagen I (C), scleraxis (D), decorin (E), and tenascin C (F) markers. A significantly higher expression can be observed in the case of scaffolds treated with BMP-12. However, an even greater improvement of the tenogenic differentiation was achieved in the case of samples subjected to a combination of mechanical and biochemical stimuli ( $n = 3$ ; significant differences: \* $p < 0.05$ , \*\* $p < 0.01$ , \*\*\* $p < 0.001$ , and \*\*\*\* $p < 0.0001$ ).

The constructs were biochemically and mechanically stimulated to mimic the natural function of tendons. The biochemical stimuli were provided by culturing the samples in 10 ng/mL BMP-12 modified culture medium. A custom-built bioreactor was used to perform the dynamic culture of the constructs. The scaffolds were mounted into the bioreactor chamber and placed and cultured in the incubator (37 °C, 5% CO<sub>2</sub>), as shown in Figure S1. Mechanical stimulation parameters were selected in terms of strain and frequency to simulate the tendon native biochemical conditions. The constructs were cultured into the bioreactor chamber and subjected to tensile cyclic loading for 7 days (4 h/day). The combination of mechanical and biochemical stimulation as well as their synergistic effect on cellular functions was evaluated. The morphology of the MSCs cultured for 7 days within the ML scaffolds was significantly affected by mechanical stimulation. The applied mechanical stimuli resulted in a longitudinal orientation of cell cytoskeletons as demonstrated by F-actin fluorescence images (Figures 4A and S3). The alignment quantifications are reported in Figures 4B and S4 for various culture conditions. Cells cultured in dynamic condition (DC) tended to align in the direction of the applied strain up to 40%, while cells cultured in static condition (SC) showed random orientation.

Additionally, the maturation and function of the cultured cells were investigated under biochemical and mechanical stimuli. The expression of collagen I, as the main component of native tendon ECM, was assessed by staining against the protein. The biochemical stimulation of the cultures resulted in a significant enhancement of collagen I production while the mechanical input promoted a more organized and oriented collagen expression, as shown in Figure S5. On the other hand, the mechanical stimulation showed a positive impact on proliferation rate of the cultured cells over time (Figure 5A), suggesting that dynamic culture condition supported cell viability and promoted cell proliferation, as also reported by previous studies.<sup>50</sup> Interestingly, the combination of mechanical and

biochemical stimuli resulted in higher cellular proliferation in comparison to the cultures that were exposed to a single stimulation.

The influence of the applied mechanical strain on MSCs cultured into the ML scaffolds was investigated in terms of potential tenogenic differentiation. The gene expression of the specific tenogenic markers such as tenomodulin, collagen I, scleraxis, decorin, and tenascin C was analyzed to evaluate the cell differentiation under dynamic culture conditions, as already assessed in previous studies.<sup>49,62–64</sup> The results indicated a significant enhancement of the tenogenic differentiation of cells cultured under dynamic conditions. Moreover, it was observed that the combination of mechanical and biochemical stimuli induced a synergistic effect, which further improved the tenogenic gene expression (Figure 5B–F).

## DISCUSSION

Tendons are highly organized tissues formed from aligned fibrillar collagen fibers. To recapitulate this fibrous architecture, substrates made of nanofibers were generated using electrospinning of PCL–PA6. Electrospun constructs are mechanically strong and are easy-to-suture during surgical implantation. However, PCL–PA6 constructs are noted to be hydrophobic and do not possess biological cell binding motifs.<sup>20</sup> To create an environment suitable for cellular growth, the substrates were coated with layers of cell-laden GelMA–Alg hydrogel. Alg was used for two reasons: (1) Alg facilitated the formation of a uniform hydrogel layer on the electrospun substrates; (2) a niche formed from polysaccharides and proteins similar to native ECM was created. More in detail, alginate was introduced into the hydrogel composition to allow the fabrication of a hydrogel layer with uniform thickness. In this approach, the substrates were dip coated with hydrogel and fast cross-linking of the hydrogel layer was important to preserve its uniform thickness. The presence of alginate enabled the rapid cross-linking of the hydrogel layer by CaCl<sub>2</sub> and physically entrapping GelMA prepolymers. GelMA was then cross-linked using UV

light to form an independent polymeric network. GelMA possesses cell binding moieties and has been successfully used for culture of various tissues.<sup>27,53,65,66</sup> Previously, it was demonstrated that alginate at concentrations lower than 1% (w/v) does not significantly affect the cell–GelMA interactions.<sup>10,22</sup> The engineered composite platform was comprised of multiple compartments that can be independently tailored. The nanofibrous substrate provided the mechanical support to the scaffold and facilitated the implantation of the constructs at the injury site. The ML scaffold has the novelty to independently make the optimization of each compartment possible. Thus, it is possible to encapsulate cells in a cell-friendly environment, which can emulate the ECM ambience, while having adequate mechanical properties for the application. Moreover, the presence of the electrospun mat can potentially facilitate the *in vivo* implantation, which would not be possible using hydrogel-based scaffolds.

Recently, a method was developed by Tamayol et al. enabling the fabrication of stable structures from various proteins in which Alg was used to form a stable template entrapping protein chains until they were properly cross-linked.<sup>61,67</sup>

The polymer concentration and the electrospinning parameters were optimized to produce electrospun structures, which provide mechanical properties that can support the proper function of scaffolds designed for the repair of injured sites of tendon tissue. The mechanical properties were measured in two directions. In the lateral direction, the electrospun substrate acted as a reinforcement. Since the tensile modulus of the fibrous substrate was significantly higher than the hydrogel layer, no significant change was observed after the addition of the hydrogel layer. Particularly, the value of ultimate tensile stress is comparable with native tendons data previously reported in the literature,<sup>68</sup> showing the suitability of the scaffold for tendon applications. On the other hand, in the perpendicular direction, the mechanical load was mainly absorbed by the hydrogel layers and a significant difference between the measured perpendicular compressive and lateral tensile moduli was observed: higher Alg concentration led to higher compression properties because of the formation of interpenetrating network hydrogels with stiffer structures.<sup>65</sup> For this reason, the hydrogel composition could significantly affect the mechanical properties in the perpendicular direction without affecting the properties in the lateral direction.

The rate of tenogenesis is slow, and a suitable scaffold should remain stable until the new tissues have deposited strong ECM to withstand the exerted mechanical forces. Although the scaffolds had multicompartments with different compositions, the focus of the degradation experiment was the reinforcing nanofibrous substrate. The degradation of polymeric substrate is mainly due to hydrolysis, and we used PBS, which captures the physiological properties of the native tissues. The degradation of GelMA is enzymatic, as it has been reported in several studies.<sup>27,69–71</sup> Additionally, hydrolysis of the Alg component also influenced the weight loss of the final ML structures, and higher Alg concentration formed scaffolds more resistant to *in vitro* degradation conditions. On the other hand, softer gels swelled easier and lower concentrations of Alg resulted in higher swelling ratio, due to the less dense and weaker polymeric networks, which can accommodate more water molecules, leading to higher fluid loading capacity.<sup>72</sup>

The biological characterization of the scaffolds showed that cellular growth and proliferation of MSCs were registered to be significantly higher into ML scaffolds having lower Alg

concentration. The observed trend in cellular growth was due to the formation of stiffer and denser hydrogels at higher concentrations of Alg, which did not favor cell migration, spreading, and proliferation.<sup>61</sup>

Tendons undergo mechanical loading during its physiological operation, and there are a number of studies suggesting the positive role of mechanical stimulation on cellular alignment and differentiation.<sup>56,57,73</sup> However, the synergistic effect of BMP-12 and mechanical stimulation on cellular growth, morphology, and differentiation is not well understood in the literature. To understand the relative and synergistic effect of biochemical and mechanical stimulation, the constructs were biochemically and mechanically stimulated to mimic the natural function of tendon and simulate its native biochemical conditions. Dynamic culture conditions showed a positive effect on cellular proliferation, according to previous studies.<sup>50</sup> Interestingly, the combination of mechanical and biochemical stimuli resulted in higher cellular proliferation in comparison to the cultures that were exposed to a single stimulation. Moreover, mechanical tensile stretching conditions led to cellular integrin-mediated focal adhesions and cytoskeleton deformation response, which resulted in a preferential, longitudinal cell orientation. Since that electrospun fibrous mat had a random fibers distribution, it was postulated that cell alignment was not related to the morphology and architecture of the fibrous substrate. Thus, the observed changes in the cellular alignment probably was due to the cyclic mechanical tensile stimulation of the cultures. The mechanical stimulation should have promoted cellular reorganization in the direction of the stretching, as it has also been observed in previous studies.<sup>50,51</sup> Additionally, collagen I expression was assessed in order to evaluate the ECM deposition. The greater expression of collagen I demonstrated the higher ECM production and deposition by cells treated with BMP-12. The mechanical input, however, promoted a more organized and oriented collagen production, mimicking the natural tendon ECM structure. Results were in agreement with previous works that demonstrated the alignment of collagen and ECM deposition under mechanical tensile stretching conditions.<sup>51</sup>

A significant enhancement of the tenogenic differentiation of cells cultured under dynamic conditions was also observed.<sup>49,64,74</sup> However, it was observed that the combination of mechanical and biochemical stimuli induced a synergistic effect, which further improved the tenogenic gene expression, confirming the positive role of BMP-12 on tenogenic differentiation without exerting an inhibitory effect at the studied range.<sup>42,55,75</sup> The simultaneous biochemical and mechanical stimulation results in a significantly higher expression level of tenogenic specific markers compared to the nonstimulated culture condition, suggesting that the proposed 3D ML system can be potentially used for engineering of functional tendons.

One of the limitations of the proposed approach was the need for *in vitro* maturation of the cultured tissues prior to implantation. This means that the patients should suffer from complications associated to the injury prior to maturation of the tissue. However, the applied mechanical stimulations were selected to recapitulate the mechanical stresses applied to tendon tissues. Thus, it is expected that an unmaturing tissue can still receive sufficient mechanical cues postimplantation to mature *in vivo*.

Moreover, the scaffold we proposed requires the treatment with GFs supplemented in the culture media, in order to improve the tenogenic differentiation of the encapsulated cells. The possibility of loading GFs into the electrospun mat or

binding them to the hydrogel backbone enable the implantation of the construct prior to cellular differentiation.

## CONCLUSIONS

In this work, we designed and fabricated 3D ML scaffolds formed from electrospun nanofibrous substrates coated by thin layers of cell-laden hydrogel for tendon regeneration. The composition of the hydrogel was tailored independently to ensure proper support for cellular growth and differentiation. The scaffolds were both biochemically and mechanically stimulated. The concentration of the chemical stimulus (BMP-12) was selected to facilitate tenogenic differentiation of MSCs. The cultures were mechanically stimulated in a bioreactor showing the positive role of the tested dynamic culture condition on cell alignment and tenogenic differentiation. Our results also demonstrated that the addition of the selected amount of BMP-12 (10 ng/mL) induces tenogenic differentiation more effectively during dynamic stimulation compared to static conditions. The synergistic effect of mechanical and biochemical stimulation results in an enhancement of cell adhesion, proliferation, alignment, and differentiation, illustrating the potential of the scaffold and the bioreactor system for tendon tissue engineering. These results provide insight on selection of proper culture conditions for engineering highly organized and biomimetic tendon tissues. In addition, the proposed ML constructs in which each compartment can be independently tailored paves the way for engineering tissue-like constructs with suitable mechanical properties at both tissue and cell levels. Further investigations are required to validate the possibility of loading GFs into the scaffold components to facilitate the tissue integration upon its implantation, which is essential for the potential clinical translation of the system.

## ASSOCIATED CONTENT

### Supporting Information

The Supporting Information is available free of charge on the ACS Publications website at DOI: [10.1021/acsbomaterials.8b01647](https://doi.org/10.1021/acsbomaterials.8b01647).

Figure S1, bioreactor model; Figure S2, fluorescence images of alive and dead cells cultured into ML scaffolds; Figure S3, fluorescence images of the cell cytoskeletons of MSCs encapsulated into ML scaffolds; Figure S4, quantification of the average alignment angle of MSCs within the ML scaffolds; Figure S5, collagen I expression by MSCs encapsulated into ML scaffolds (PDF)

## AUTHOR INFORMATION

### Corresponding Authors

\*E-mail: [atamayol@unl.edu](mailto:atamayol@unl.edu) (A. Tamayol).

\*E-mail: [wojciech.swieszkowski@pw.edu.pl](mailto:wojciech.swieszkowski@pw.edu.pl) (W.S.).

\*E-mail: [khademh@ucla.edu](mailto:khademh@ucla.edu) (A.K.).

### ORCID

Abuduwaili Tuoheti: 0000-0003-0647-2212

Nasim Annabi: 0000-0003-1879-1202

Ali Khademhosseini: 0000-0002-2692-1524

Ali Tamayol: 0000-0003-1801-2889

### Notes

The authors declare no competing financial interest.

## ACKNOWLEDGMENTS

This study was supported by the National Center for Research and Development (STRATEGMED1/233224/10/NCBR/2014, project START). This research has been partially supported by the National Institutes of Health (HL092836, DE019024, EB012597, AR057837, DE021468, HL099073, EB008392, GM126831, AR073822). A. Tamayol acknowledges the financial support from the University of Nebraska, Lincoln, and Nebraska Tobacco Settlement Biomedical Research Enhancement Funds. I.K.Y. acknowledges financial support from the National Institutes of Health (5T32EB016652, 1T32EB016652). G.T.d.S. gratefully acknowledges the funding received by CONACyT (scholarship 234713) and Fundación México in Harvard in the form of postdoctoral scholarships. This research has been partially funded by the Tec de Monterrey and MIT Nanotechnology Program and the MIT International Science and Technology Initiatives (MISTI).

## REFERENCES

- (1) James, R.; Kesturu, G.; Balian, G.; Chhabra, A. B. Tendon: biology, biomechanics, repair, growth factors, and evolving treatment options. *J. Hand Surg Am.* **2008**, *33* (1), 102–12.
- (2) Ratcliffe, A.; Butler, D. L.; Dymott, N. A.; Cagle, P. J., Jr.; Proctor, C. S.; Ratcliffe, S. S.; Flatow, E. L. Scaffolds for tendon and ligament repair and regeneration. *Ann. Biomed. Eng.* **2015**, *43* (3), 819–31.
- (3) Andarawis-Puri, N.; Flatow, E. L.; Soslowsky, L. J. Tendon basic science: Development, repair, regeneration, and healing. *J. Orthop. Res.* **2015**, *33* (6), 780–4.
- (4) Hoffmann, A.; Gross, G. Tendon and ligament engineering: from cell biology to in vivo application. *Regener. Med.* **2006**, *1* (4), 563–74.
- (5) Longo, U. G.; Lamberti, A.; Maffulli, N.; Denaro, V. Tendon augmentation grafts: a systematic review. *Br. Med. Bull.* **2010**, *94*, 165–88.
- (6) Leong, N. L.; Petrigliano, F. A.; McAllister, D. R. Current tissue engineering strategies in anterior cruciate ligament reconstruction. *J. Biomed. Mater. Res., Part A* **2014**, *102* (5), 1614–24.
- (7) Idaszek, J.; Kijewska, E.; Łojkowski, M.; Swieszkowski, W. How important are scaffolds and their surface properties in regenerative medicine. *Appl. Surf. Sci.* **2016**, *388* (Part B), 762–774.
- (8) Tamayol, A.; Akbari, M.; Annabi, N.; Paul, A.; Khademhosseini, A.; Juncker, D. Fiber-based tissue engineering: Progress, challenges, and opportunities. *Biotechnol. Adv.* **2013**, *31* (5), 669–87.
- (9) Kijewska, E.; Swieszkowski, W. 2 - General requirements of electrospun materials for tissue engineering: Setups and strategy for successful electrospinning in laboratory and industry. In *Electrospun Materials for Tissue Engineering and Biomedical Applications*; Kny, E., Ed.; Woodhead Publishing, 2017; pp 43–56; DOI: [10.1016/B978-0-08-101022-8.00002-8](https://doi.org/10.1016/B978-0-08-101022-8.00002-8).
- (10) Costa-Almeida, R.; Domingues, R. M. A.; Fallahi, A.; Avci, H.; Yazdi, I. K.; Akbari, M.; Reis, R. L.; Tamayol, A.; Gomes, M. E.; Khademhosseini, A. Cell-laden composite suture threads for repairing damaged tendons. *J. Tissue Eng. Regener. Med.* **2018**, *12* (4), 1039–1048.
- (11) Bhardwaj, N.; Kundu, S. C. Electrospinning: a fascinating fiber fabrication technique. *Biotechnol. Adv.* **2010**, *28* (3), 325–47.
- (12) Moffat, K. L.; Kwei, A. S.; Spalazzi, J. P.; Doty, S. B.; Levine, W. N.; Lu, H. H. Novel nanofiber-based scaffold for rotator cuff repair and augmentation. *Tissue Eng., Part A* **2009**, *15* (1), 115–26.
- (13) Mauck, R. L.; Baker, B. M.; Nerurkar, N. L.; Burdick, J. A.; Li, W. J.; Tuan, R. S.; Elliott, D. M. Engineering on the straight and narrow: the mechanics of nanofibrous assemblies for fiber-reinforced tissue regeneration. *Tissue Eng., Part B* **2009**, *15* (2), 171–93.
- (14) Rinoldi, C.; Kijewska, E.; Chlanda, A.; Choinska, E.; Khenoussi, N.; Tamayol, A.; Khademhosseini, A.; Swieszkowski, W. Nanobead-on-string composites for tendon tissue engineering. *J. Mater. Chem. B* **2018**, *6* (19), 3116–3127.

- (15) Nasajpour, A.; Mandla, S.; Shree, S.; Mostafavi, E.; Sharifi, R.; Khalilpour, A.; Saghadzadeh, S.; Hassan, S.; Mitchell, M. J.; Leijten, J.; Hou, X.; Moshaverinia, A.; Annabi, N.; Adelung, R.; Mishra, Y. K.; Shin, S. R.; Tamayol, A.; Khademhosseini, A. Nanostructured Fibrous Membranes with Rose Spike-Like Architecture. *Nano Lett.* **2017**, *17* (10), 6235–6240.
- (16) Nasajpour, A.; Ansari, S.; Rinoldi, C.; Rad, A. S.; Aghaloo, T.; Shin, S. R.; Mishra, Y. K.; Adelung, R.; Swieszkowski, W.; Annabi, N.; Khademhosseini, A.; Moshaverinia, A.; Tamayol, A. A Multifunctional Polymeric Periodontal Membrane with Osteogenic and Antibacterial Characteristics. *Adv. Funct. Mater.* **2018**, *28* (3), 1703437.
- (17) Kijenska, E.; Zhang, S.; Prabhakaran, M. P.; Ramakrishna, S.; Swieszkowski, W. Nanoengineered biocomposite tricomponent polymer based matrices for bone tissue engineering. *Int. J. Polym. Mater.* **2016**, *65* (16), 807–815.
- (18) Manning, C. N.; Schwartz, A. G.; Liu, W.; Xie, J.; Havlioglu, N.; Sakiyama-Elbert, S. E.; Silva, M. J.; Xia, Y.; Gelberman, R. H.; Thomopoulos, S. Controlled delivery of mesenchymal stem cells and growth factors using a nanofiber scaffold for tendon repair. *Acta Biomater.* **2013**, *9* (6), 6905–6914.
- (19) Jin, H. J.; Chen, J.; Karageorgiu, V.; Altman, G. H.; Kaplan, D. L. Human bone marrow stromal cell responses on electrospun silk fibroin mats. *Biomaterials* **2004**, *25* (6), 1039–47.
- (20) Yang, G.; Lin, H.; Rothrauff, B. B.; Yu, S.; Tuan, R. S. Multilayered polycaprolactone/gelatin fiber-hydrogel composite for tendon tissue engineering. *Acta Biomater.* **2016**, *35*, 68–76.
- (21) Bettahalli, N. M.; Groen, N.; Steg, H.; Unadkat, H.; de Boer, J.; van Blitterswijk, C. A.; Wessling, M.; Stamatialis, D. Development of multilayer constructs for tissue engineering. *J. Tissue Eng. Regen. Med.* **2014**, *8* (2), 106–19.
- (22) Akbari, M.; Tamayol, A.; Laforte, V.; Annabi, N.; Najafabadi, A. H.; Khademhosseini, A.; Juncker, D. Composite Living Fibers for Creating Tissue Constructs Using Textile Techniques. *Adv. Funct. Mater.* **2014**, *24* (26), 4060–4067.
- (23) Eslami, M.; Vrana, N. E.; Zorlutuna, P.; Sant, S.; Jung, S.; Masoumi, N.; Khavari-Nejad, R. A.; Javadi, G.; Khademhosseini, A. Fiber-reinforced hydrogel scaffolds for heart valve tissue engineering. *J. Biomater. Appl.* **2014**, *29* (3), 399–410.
- (24) Kosik-Koziol, A.; Costantini, M.; Bolek, T.; Szoke, K.; Barbetta, A.; Brinchmann, J.; Swieszkowski, W. PLA short sub-micron fiber reinforcement of 3D bioprinted alginate constructs for cartilage regeneration. *Biofabrication* **2017**, *9* (4), No. 044105.
- (25) Chainani, A.; Hippensteel, K. J.; Kishan, A.; Garrigues, N. W.; Ruch, D. S.; Guilak, F.; Little, D. Multilayered electrospun scaffolds for tendon tissue engineering. *Tissue Eng., Part A* **2013**, *19* (23–24), 2594–604.
- (26) Celikkin, N.; Rinoldi, C.; Costantini, M.; Trombetta, M.; Rainer, A.; Swieszkowski, W. Naturally derived proteins and glycosaminoglycan scaffolds for tissue engineering applications. *Mater. Sci. Eng., C* **2017**, *78*, 1277–1299.
- (27) Yue, K.; Trujillo-de Santiago, G.; Alvarez, M. M.; Tamayol, A.; Annabi, N.; Khademhosseini, A. Synthesis, properties, and biomedical applications of gelatin methacryloyl (GelMA) hydrogels. *Biomaterials* **2015**, *73*, 254–71.
- (28) Costantini, M.; Idaszek, J.; Szoke, K.; Jaroszewicz, J.; Dentini, M.; Barbetta, A.; Brinchmann, J. E.; Swieszkowski, W. 3D bioprinting of BM-MSCs-loaded ECM biomimetic hydrogels for in vitro neocartilage formation. *Biofabrication* **2016**, *8* (3), 035002.
- (29) Rezaei Nejad, H.; Goli Malekabadi, Z.; Kazemzadeh Narbat, M.; Annabi, N.; Mostafalu, P.; Tarlan, F.; Zhang, Y. S.; Hoorfar, M.; Tamayol, A.; Khademhosseini, A. Laterally Confined Microfluidic Patterning of Cells for Engineering Spatially Defined Vascularization. *Small* **2016**, *12* (37), 5132–5139.
- (30) Lui, P. P. Stem cell technology for tendon regeneration: current status, challenges, and future research directions. *Stem Cells Cloning: Adv. Appl.* **2015**, *8*, 163–74.
- (31) MacLean, S.; Khan, W. S.; Malik, A. A.; Snow, M.; Anand, S. Tendon regeneration and repair with stem cells. *Stem Cells Int.* **2012**, *2012*, 316281.
- (32) Knight, M. N.; Hankenson, K. D. Mesenchymal Stem Cells in Bone Regeneration. *Adv. Wound Care (New Rochelle)* **2013**, *2* (6), 306–316.
- (33) Zhao, S.; Zhao, J.; Dong, S.; Huangfu, X.; Li, B.; Yang, H.; Zhao, J.; Cui, W. Biological augmentation of rotator cuff repair using bFGF-loaded electrospun poly(lactide-co-glycolide) fibrous membranes. *Int. J. Nanomed.* **2014**, *9*, 2373–85.
- (34) Cheng, X.; Tsao, C.; Sylvia, V. L.; Cornet, D.; Nicoletta, D. P.; Bredbenner, T. L.; Christy, R. J. Platelet-derived growth-factor-releasing aligned collagen-nanoparticle fibers promote the proliferation and tenogenic differentiation of adipose-derived stem cells. *Acta Biomater.* **2014**, *10* (3), 1360–9.
- (35) Testa, S.; Costantini, M.; Fornetti, E.; Bernardini, S.; Trombetta, M.; Seliktar, D.; Cannata, S.; Rainer, A.; Gargioli, C. Combination of biochemical and mechanical cues for tendon tissue engineering. *J. Cell Mol. Med.* **2017**, *21* (11), 2711–2719.
- (36) Goncalves, A. I.; Rodrigues, M. T.; Lee, S. J.; Atala, A.; Yoo, J. J.; Reis, R. L.; Gomes, M. E. Understanding the role of growth factors in modulating stem cell tenogenesis. *PLoS One* **2013**, *8* (12), No. e83734.
- (37) Shen, H.; Gelberman, R. H.; Silva, M. J.; Sakiyama-Elbert, S. E.; Thomopoulos, S. BMP12 induces tenogenic differentiation of adipose-derived stromal cells. *PLoS One* **2013**, *8* (10), No. e77613.
- (38) Rinoldi, C.; Costantini, M.; Kijenska-Gawronska, E.; Testa, S.; Fornetti, E.; Heljak, M.; Cwiklinska, M.; Buda, R.; Baldi, J.; Cannata, S.; Guzowski, J.; Gargioli, C.; Khademhosseini, A.; Swieszkowski, W. Tendon Tissue Engineering: Effects of Mechanical and Biochemical Stimulation on Stem Cell Alignment on Cell-Laden Hydrogel Yarns. *Adv. Healthcare Mater.* **2019**, *8*, 1801218.
- (39) Park, A.; Hogan, M. V.; Kesturu, G. S.; James, R.; Balian, G.; Chhabra, A. B. Adipose-derived mesenchymal stem cells treated with growth differentiation factor-5 express tendon-specific markers. *Tissue Eng., Part A* **2010**, *16* (9), 2941–51.
- (40) Kuo, C. K.; Tuan, R. S. Mechanoactive tenogenic differentiation of human mesenchymal stem cells. *Tissue Eng., Part A* **2008**, *14* (10), 1615–27.
- (41) Francis-West, P. H.; Parish, J.; Lee, K.; Archer, C. W. BMP/GDF-signalling interactions during synovial joint development. *Cell Tissue Res.* **1999**, *296* (1), 111–119.
- (42) Violini, S.; Ramelli, P.; Pisani, L. F.; Gorni, C.; Mariani, P. Horse bone marrow mesenchymal stem cells express embryo stem cell markers and show the ability for tenogenic differentiation by in vitro exposure to BMP-12. *BMC Cell Biol.* **2009**, *10*, 29.
- (43) Lee, J. Y.; Zhou, Z.; Taub, P. J.; Ramcharan, M.; Li, Y.; Akinbiyi, T.; Maharam, E. R.; Leong, D. J.; Laudier, D. M.; Ruike, T.; Torina, P. J.; Zaidi, M.; Majeska, R. J.; Schaffler, M. B.; Flatow, E. L.; Sun, H. B. BMP-12 treatment of adult mesenchymal stem cells in vitro augments tendon-like tissue formation and defect repair in vivo. *PLoS One* **2011**, *6* (3), No. e17531.
- (44) Zarychta-Wisniewska, W.; Burdzinska, A.; Kulesza, A.; Gala, K.; Kaleta, B.; Zielniok, K.; Siennicka, K.; Sabat, M.; Paczek, L. Bmp-12 activates tenogenic pathway in human adipose stem cells and affects their immunomodulatory and secretory properties. *BMC Cell Biol.* **2017**, *18* (1), 13.
- (45) Gelberman, R. H.; Shen, H.; Kormpakis, I.; Rothrauff, B.; Yang, G.; Tuan, R. S.; Xia, Y.; Sakiyama-Elbert, S.; Silva, M. J.; Thomopoulos, S. Effect of adipose-derived stromal cells and BMP12 on intrasynovial tendon repair: A biomechanical, biochemical, and proteomics study. *J. Orthop. Res.* **2016**, *34* (4), 630–640.
- (46) Liu, Y.; Suen, C.-W.; Zhang, J.-f.; Li, G. Current concepts on tenogenic differentiation and clinical applications. *Journal of Orthopaedic Translation* **2017**, *9*, 28–42.
- (47) Greiner, S.; Ide, J.; Van Noort, A.; Mochizuki, Y.; Ochi, H.; Marraffino, S.; Sridharan, S.; Rudicel, S.; Itoi, E. Local rhBMP-12 on an Absorbable Collagen Sponge as an Adjuvant Therapy for Rotator Cuff Repair - A Phase I, Randomized, Standard of Care Control, Multicenter Study: Safety and Feasibility. *Am. J. Sports Med.* **2015**, *43* (8), 1994–2004.
- (48) Jelinsky, S. A.; Li, L.; Ellis, D.; Archambault, J.; Li, J.; St. Andre, M.; Morris, C.; Seeherman, H. Treatment with rhBMP12 or rhBMP13

increase the rate and the quality of rat Achilles tendon repair. *J. Orthop. Res.* **2011**, *29* (10), 1604–12.

(49) Youngstrom, D. W.; Rajpar, I.; Kaplan, D. L.; Barrett, J. G. A bioreactor system for in vitro tendon differentiation and tendon tissue engineering. *J. Orthop. Res.* **2015**, *33* (6), 911–8.

(50) Wu, S.; Wang, Y.; Streubel, P. N.; Duan, B. Living nanofiber yarn-based woven biotextiles for tendon tissue engineering using cell triculture and mechanical stimulation. *Acta Biomater.* **2017**, *62* (Supplement C), 102–115.

(51) Wang, J. H.; Yang, G.; Li, Z.; Shen, W. Fibroblast responses to cyclic mechanical stretching depend on cell orientation to the stretching direction. *J. Biomech.* **2004**, *37* (4), 573.

(52) Aubin, H.; Nichol, J. W.; Hutson, C. B.; Bae, H.; Sieminski, A. L.; Cropek, D. M.; Akhyari, P.; Khademhosseini, A. Directed 3D cell alignment and elongation in microengineered hydrogels. *Biomaterials* **2010**, *31* (27), 6941–6951.

(53) Byambaa, B.; Annabi, N.; Yue, K.; Trujillo-de Santiago, G.; Alvarez, M. M.; Jia, W.; Kazemzadeh-Narbat, M.; Shin, S. R.; Tamayol, A.; Khademhosseini, A. Bioprinted Osteogenic and Vasculogenic Patterns for Engineering 3D Bone Tissue. *Adv. Healthcare Mater.* **2017**, *6* (16), 1700015.

(54) Beitzel, K.; McCarthy, M. B.; Cote, M. P.; Russell, R. P.; Apostolakis, J.; Ramos, D. M.; Kumbar, S. G.; Imhoff, A. B.; Arciero, R. A.; Mazzocca, A. D. Properties of biologic scaffolds and their response to mesenchymal stem cells. *Arthroscopy* **2014**, *30* (3), 289–98.

(55) Fu, S. C.; Wong, Y. P.; Chan, B. P.; Pau, H. M.; Cheuk, Y. C.; Lee, K. M.; Chan, K. M. The roles of bone morphogenetic protein (BMP) 12 in stimulating the proliferation and matrix production of human patellar tendon fibroblasts. *Life Sci.* **2003**, *72* (26), 2965–74.

(56) Skuttek, M.; Griensven, M.; Zeichen, J.; Brauer, N.; Bosch, U. Cyclic mechanical stretching modulates secretion pattern of growth factors in human tendon fibroblasts. *Eur. J. Appl. Physiol.* **2001**, *86* (1), 48–52.

(57) Galloway, M. T.; Lalley, A. L.; Shearn, J. T. The role of mechanical loading in tendon development, maintenance, injury, and repair. *J. Bone Joint Surg Am.* **2013**, *95* (17), 1620–8.

(58) Ulery, B. D.; Nair, L. S.; Laurencin, C. T. Biomedical Applications of Biodegradable Polymers. *J. Polym. Sci., Part B: Polym. Phys.* **2011**, *49* (12), 832–864.

(59) Chlanda, A.; Kijenska, E.; Rinoldi, C.; Tarnowski, M.; Wierzchon, T.; Swieszkowski, W. Structure and physico-mechanical properties of low temperature plasma treated electrospun nanofibrous scaffolds examined with atomic force microscopy. *Micron* **2018**, *107*, 79–84.

(60) Angeloni, V.; Contessi, N.; De Marco, C.; Bertoldi, S.; Tanzi, M. C.; Daidone, M. G.; Farè, S. Polyurethane foam scaffold as in vitro model for breast cancer bone metastasis. *Acta Biomater.* **2017**, *63*, 306–316.

(61) Tamayol, A.; Najafabadi, A. H.; Aliakbarian, B.; Arab-Tehrany, E.; Akbari, M.; Annabi, N.; Juncker, D.; Khademhosseini, A. Hydrogel Templates for Rapid Manufacturing of Bioactive Fibers and 3D Constructs. *Adv. Healthcare Mater.* **2015**, *4* (14), 2146–2153.

(62) Qin, T. W.; Sun, Y. L.; Thoreson, A. R.; Steinmann, S. P.; Amadio, P. C.; An, K. N.; Zhao, C. Effect of mechanical stimulation on bone marrow stromal cell-seeded tendon slice constructs: a potential engineered tendon patch for rotator cuff repair. *Biomaterials* **2015**, *51*, 43–50.

(63) Burk, J.; Plenge, A.; Brehm, W.; Heller, S.; Pfeiffer, B.; Kasper, C. Induction of Tenogenic Differentiation Mediated by Extracellular Tendon Matrix and Short-Term Cyclic Stretching. *Stem Cells Int.* **2016**, *2016*, 7342379.

(64) Doroski, D. M.; Levenston, M. E.; Temenoff, J. S. Cyclic tensile culture promotes fibroblastic differentiation of marrow stromal cells encapsulated in poly(ethylene glycol)-based hydrogels. *Tissue Eng., Part A* **2010**, *16* (11), 3457–66.

(65) Celikkin, N.; Mastrogiacomo, S.; Jaroszewicz, J.; Walboomers, X. F.; Swieszkowski, W. Gelatin methacrylate scaffold for bone tissue engineering: The influence of polymer concentration. *J. Biomed. Mater. Res., Part A* **2018**, *106* (1), 201–209.

(66) Noshadi, I.; Hong, S.; Sullivan, K. E.; Shirzaei Sani, E.; Portillo-Lara, R.; Tamayol, A.; Shin, S. R.; Gao, A. E.; Stoppel, W. L.; Black, L. D., III; Khademhosseini, A.; Annabi, N. In vitro and in vivo analysis of visible light crosslinkable gelatin methacryloyl (GelMA) hydrogels. *Biomater. Sci.* **2017**, *5* (10), 2093–2105.

(67) Tamayol, A.; Najafabadi, A. H.; Aliakbarian, B.; Arab-Tehrany, E.; Akbari, M.; Annabi, N.; Juncker, D.; Khademhosseini, A. Alginate as a template forming material for creating IPN hydrogel fibers. *J. Tissue Eng. Regen. Med.* **2014**, *8*, 314–342.

(68) Itoi, E.; Berglund, L. J.; Grabowski, J. J.; Schultz, F. M.; Grownay, E. S.; Morrey, B. F.; An, K. N. Tensile properties of the supraspinatus tendon. *J. Orthop. Res.* **1995**, *13* (4), 578–84.

(69) Suo, H.; Zhang, D.; Yin, J.; Qian, J.; Wu, Z. L.; Fu, J. Interpenetrating polymer network hydrogels composed of chitosan and photocrosslinkable gelatin with enhanced mechanical properties for tissue engineering. *Mater. Sci. Eng., C* **2018**, *92*, 612–620.

(70) Hutson, C. B.; Nichol, J. W.; Aubin, H.; Bae, H.; Yamanlar, S.; Al-Haque, S.; Koshy, S. T.; Khademhosseini, A. Synthesis and characterization of tunable poly(ethylene glycol): gelatin methacrylate composite hydrogels. *Tissue Eng., Part A* **2011**, *17* (13–14), 1713–23.

(71) Rahali, K.; Ben Messaoud, G.; Kahn, C. J. F.; Sanchez-Gonzalez, L.; Kaci, M.; Cleymand, F.; Fleutot, S.; Linder, M.; Desobry, S.; Arab-Tehrany, E. Synthesis and Characterization of Nanofunctionalized Gelatin Methacrylate Hydrogels. *Int. J. Mol. Sci.* **2017**, *18* (12), 2675.

(72) Lee, K. Y.; Mooney, D. J. Alginate: properties and biomedical applications. *Prog. Polym. Sci.* **2012**, *37* (1), 106–126.

(73) Lee, J.; Guarino, V.; Gloria, A.; Ambrosio, L.; Tae, G.; Kim, Y. H.; Jung, Y.; Kim, S. H.; Kim, S. H. Regeneration of Achilles' tendon: the role of dynamic stimulation for enhanced cell proliferation and mechanical properties. *J. Biomater. Sci., Polym. Ed.* **2010**, *21* (8–9), 1173–90.

(74) Subramony, S. D.; Dargis, B. R.; Castillo, M.; Azeloglu, E. U.; Tracey, M. S.; Su, A.; Lu, H. H. The guidance of stem cell differentiation by substrate alignment and mechanical stimulation. *Biomaterials* **2013**, *34* (8), 1942–53.

(75) Wang, Q. W.; Chen, Z. L.; Piao, Y. J. Mesenchymal stem cells differentiate into tenocytes by bone morphogenetic protein (BMP) 12 gene transfer. *J. Biosci Bioeng* **2005**, *100* (4), 418–22.